

Supporting Information

Development of Ru-polypyridyl complexes for real-time monitoring of A β oligomers and inhibition of A β fibrils formation

Xian Chen^a, Jiaoyang Wang^a, Zhenzhuo Mo^a, Lu Han^a, Kaiqing Cheng^a, Cheng Xie^c, Genyan

Liu^{c*}, Lijun Jiang^{b*}, Kai Wang^{a*}, Jie Pan^{a*}

a. College of Health Science and Engineering, Hubei University, Wuhan 430062, P. R. China

b. College of Life Sciences, Central China Normal University, Wuhan 430062, P. R. China.

c. Hubei Key Laboratory of Novel Reactor and Green Chemical Technology, School of Chemical Engineering and Pharmacy, Wuhan Institute of Technology, Wuhan, 430205, PR China

***Corresponding author.**

* E-mail address: Dr. Genyan Liu: liugenyan@wit.edu.cn

Dr. Lijun Jiang: lijunjiang@ccnu.edu.cn

Dr. Kai Wang: kaiwang@hubu.edu.cn

Dr. Jie Pan: j.pan@hubu.edu.cn

Contents

1. Materials and methods	S-4
2. Synthetic works	S-5
2.1 Synthesis of compound 1	S-5
2.2 Synthesis of compound 2	S-6
2.3 Synthesis of compound 3	S-6
2.4 Synthesis of compound 4	S-7
2.5 Synthesis of compound 5	S-7
2.6 Synthesis of compound Ru-YH	S-8
2.7 Synthesis of compound 6	S-8
2.8 Synthesis of compound 7	S-9
2.9 Synthesis of compound 8	S-9
2.10 Synthesis of compound 9	S-10
2.11 Synthesis of compound Ru-WJ	S-10
3. Analysis and detection	S-12
3.1. Measurement of photophysical properties	S-12
3.2. Preparation of A β aggregates	S-12
3.3. Quantum yield measurements	S-12
3.4. The determination of <i>pKa</i>	S-12
3.5. Log <i>P_{ow}</i> determination	S-13
3.6. Molecular docking	S-13
3.7. Fluorescence spectral measurements of Ru-WJ and Ru-YH with A β 1-42 oligomers/fibrils	S-17
3.8. Determination of the binding constant of Ru-WJ and Ru-YH for A β 1-42 aggregates.	S-14
3.9. Chemical stability of Ru-WJ and Ru-YH	S-15
3.10. Selectivity of Ru-WJ and Ru-YH	S-15
3.11. Cell culture and Cytotoxicity	S-15
3.12. TEM observation and DLS examination of A β 1-42 peptides, oligomers and fibrils	S-16

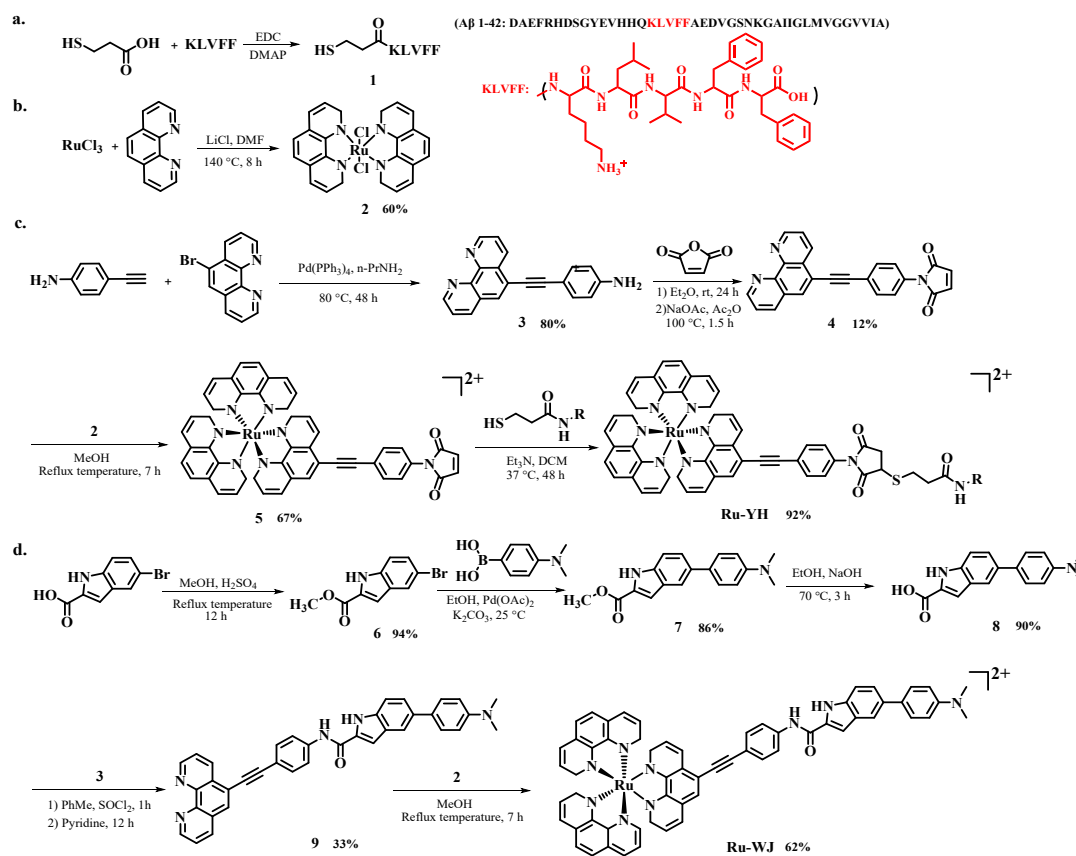
3.13. <i>Ex vivo</i> brain imaging	S-16
3.14. <i>Brain homogenate experimen and in vivo imaging</i>	S-16
4. Supporting Figures	S-18
4.1. UV-vis spectra in PBS	S-18
4.2. Spectroscopic studies of the probes versus pH.....	S-18
4.3. Chemical stability	S-19
4.4. Molecular docking analysis.....	S-19
4.5. The selectivity of Ru-WJ and Ru-YH	S-20
4.6. Binding affinity	S-20
4.7. The MTT assay of Ru-WJ and Ru-YH	S-21
4.8. ¹ H NMR, ¹³ C NMR, HPLC, HRMS and Infrared spectrum	S-21
5. References	S-32

1. Materials and methods

All solvents and chemicals were purchased from commercial suppliers in analytical grade suppliers and used directly. The A β 1-42 peptides were purchased from ChinaPeptides Company. The human cervical carcinoma cell line (HeLa), rat adrenal medullary pheochromocytoma cell line (PC12), and brain microvascular endothelial cells (bEnd.3) were purchased from the Fenghui Biology Company. The synthetic route of **Ru-WJ** and **Ru-YH** is shown in Scheme S1. All intermediates and final products were characterized by ^1H NMR, ^{13}C NMR, HPLC, and HRMS. NMR spectra were recorded on a Bruker 400 MHz (^1H : 400 MHz) spectrometer and chemical shifts were internally referenced to residual deuterium solvent. The following abbreviations were used to depict the multiplicities: s = singlet, d = doublet, t = triplet, q = quartet, dd = doublet of doublets, and m = multiplet. UV-Visible absorption spectra were recorded by a UH4150 spectrophotometer (SHIMADZU) and fluorescence measurements were carried out using a FLS1000 spectrophotometer (Edinburgh Instruments).

Ex vivo brain imaging was obtained by a confocal laser scanning microscope (Nikon ECLIPSE Ti). *In vivo* imaging was obtained on the *in vivo* fluorescence imaging system (*In-Vivo* Master).

2. Synthetic works



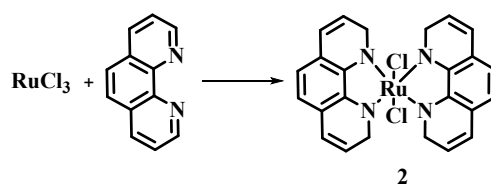
Scheme S1. Synthetic routes of Ru-YH and Ru-WJ. (R=KLVFF)

2.1 Synthesis of compound 1



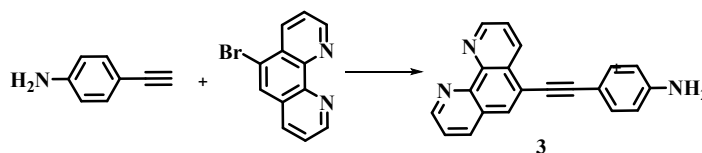
3-mercaptopropionic acid (0.5 ml), Aβ 16-20 gene sequence KLVFF (50 mg), *N*₁-((methylamino)methylene)-*N*₃, *N*₃-dimethylpropane-1, 3-diamine (EDC) (0.5 g), and 4-dimethylamino pyridine (DMAP) (0.1 g) were successively added in a 50 mL centrifuge tube. Finally, 10 ml of anhydrous dichloromethane (DCM) was added and subjected to constant temperature oscillation at 37°C for 3 days. The oil-like compound **1** was taken out and stored in a refrigerator at -20°C for use.

2.2 Synthesis of compound 2



RuCl₃·3H₂O (1.0 g, 3.8 mmol), 1,10-phenanthroline (1.4 g, 7.6 mmol), and lithium chloride (0.57 g, 2.54 mmol) were successively added in a three-necked flask under anhydrous and oxygen-free conditions. *N,N*-dimethylformamide (DMF) (10 mL) was injected and stirred vigorously at 145°C for 6 hours. After 6 hours, the mixture was cooled to room temperature, transferred to a single-ended flask, evaporated at low pressure to remove most of the DMF solvent, the remainder was cooled in ice water, and then acetone (30 mL) was added and mixed well with it. The resulting solution was placed overnight in a refrigerator at 4°C. Then, filtered and thoroughly washed with cold water (~50 mL) and ether (~20 mL), and then undergo suction drying to obtain a purplish black compound 2 (1.23 g, yield = 60%).

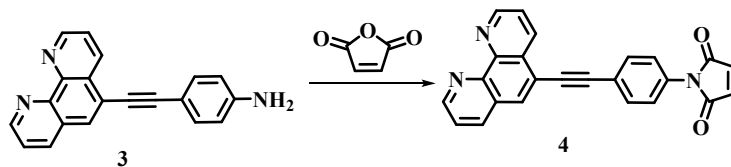
2.3 Synthesis of compound 3



4-ethynyl aniline (0.70 g, 6 mmol), 5-bromo-1,10-phenanthroline (0.74 g, 3 mmol), Pd(PPh₃)₄ (0.036 g), and *n*-propylamine (30 mL) were successively added in a pressure tube, and stirring at 80°C for two days. The resulting solution was concentrated and the residue was diluted with water (30 mL). The mixture was extracted with DCM (2×50 mL) and the combined organic layer was washed with sat. salt water (2×30 mL), dried over anhydrous Na₂SO₄ and evaporated. The crude product was purified by a chromatographic column (DCM/CH₃OH = 150:1→20:1) and yielded a pale yellow solid compound 3 (0.675 g, yield = 80%). ¹H NMR (400 MHz, DMSO-*d*₆) δ 9.13 (ddd, *J* = 33.0, 4.3, 1.7 Hz, 2H), 8.84 (dd, *J* = 8.2, 1.7 Hz, 1H), 8.48 (dd, *J* = 8.2, 1.8 Hz, 1H), 8.23 (s, 1H), 7.84 (ddd, *J* = 46.1, 8.1, 4.3 Hz, 2H), 7.58 – 7.33 (m, 2H), 6.89 – 6.52 (m, 2H), 5.74 (s, 2H). ¹³C NMR (101 MHz, DMSO-*d*₆) δ 150.72 (d, *J* = 19.2 Hz), 145.71

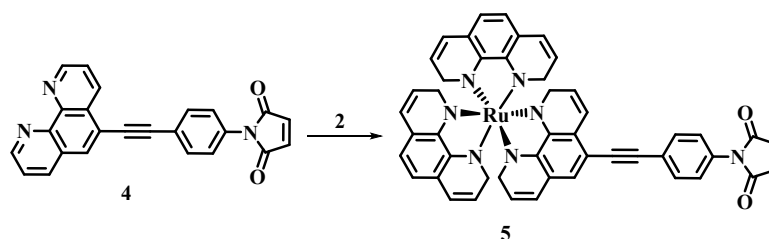
(d, $J = 32.8$ Hz), 136.41, 134.83, 133.52, 129.87, 128.37 (d, $J = 47.9$ Hz), 124.25 (d, $J = 6.9$ Hz), 120.30, 114.16, 107.87, 98.16, 83.83, 49.08.

2.4 Synthesis of compound 4



Compound **3** (0.59 g, 2.0 mmol), maleic anhydride (0.42 g, 4.0 mmol), and ether (36 ml) were successively added in a single-ended flask, and the reaction was conducted at room temperature for 24 hours. The reaction mixture was filtered and washed with ice water (10 mL) and ether (10 mL), respectively. The filter residue was dried and obtained dark yellow powder. Added the dark yellow powder to another flask, then sodium acetate (112 mg) and acetic anhydride (30 mL) were added and stirred for 1.5 hours at 80°C. The mixture was poured into a large amount of ice water at room temperature and collected as a brown solid through suction filtration. Subsequently, the brown solid was dissolved in chloroform (15 mL) and subjected to reduced pressure distillation to obtain a yellow intermediate crude product. The crude product was purified by column chromatography (DCM/CH₃OH = 80:1) to obtain a light yellow powdery compound **4** (0.09 g, yield = 12%). ¹H NMR (400 MHz, DMSO-d₆) δ 9.20 (s, 1H), 9.12 (s, 1H), 8.90 (s, 1H), 8.57 (s, 1H), 8.39 (s, 1H), 7.96 (s, 1H), 7.85 (s, 1H), 7.78 (s, 2H), 7.72 (s, 2H), 6.27 (s, 1H), 6.12 (s, 1H).

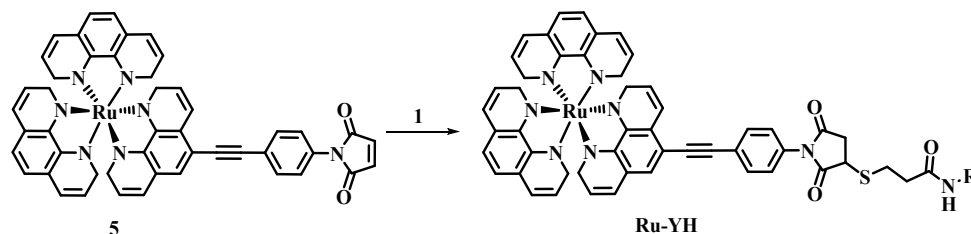
2.5 Synthesis of compound 5



Under argon protection, compound **2** (0.13 g, 0.24 mmol) and compound **4** (0.09 g, 0.24 mmol) were dissolved in methanol (MeOH) (15 mL) and reacted in a condensing device for 7 hours. After the reaction, the obtained substance was purified by column chromatography with neutral Al₂O₃ (DCM/MeOH = 50:1) to obtain an

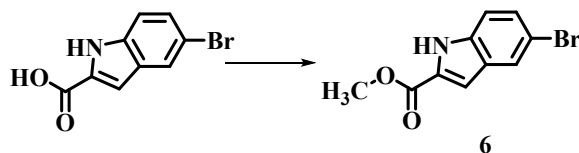
orange-red solid compound **5** (0.14 g, yield = 67%). Mass spectrometry (HRMS, m/z): $[M]^+$ calcd. for $[C_{48}H_{35}N_7O_2Ru]^+$: 843.1890; found: 843.1854.

2.6 Synthesis of compound Ru-YH



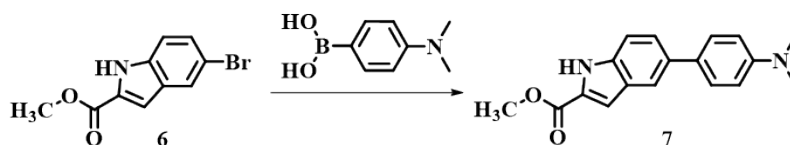
Compound **1** (0.10 g), compound **5** (0.10 g, 0.12 mmol), triethylamine (0.1 ml), and DCM (15 ml) were successively added in a 50 mL centrifuge tube. The reaction was shaken at 37°C for 2 days and followed by TLC. After the reaction, the solvent was evaporated under vacuum at 30°C to obtain an orange-red solid compound **Ru-YH** (0.17 g, yield = 92%). Mass spectrometry (HRMS, m/z): $[M]^+$ calcd. for $[C_{86}H_{92}N_{13}O_9RuS]^+$: 1583.5821; found: 1583.4630.

2.7 Synthesis of compound 6



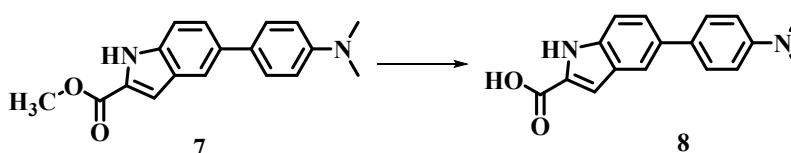
5-bromo-2-indolecarboxylic acid (1.00 g, 6.21 mmol) was dissolved in methanol (5 mL), then concentrated sulfuric acid (3 drops) was added and refluxed overnight. The resulting solution was concentrated. Then, the mixture was extracted with DCM (2×50 mL) and the combined organic layer was washed with sat. salt water (3×30 mL) and dried over anhydrous Na_2SO_4 . The solvent was removed to obtain a white solid compound **6** (0.94 g, yield = 94%). 1H NMR (400 MHz, $DMSO-d_6$) δ 12.15 (s, 1H), 7.89 (d, $J = 1.8$ Hz, 1H), 7.59 – 7.28 (m, 2H), 7.14 (dd, $J = 2.2, 0.8$ Hz, 1H), 3.88 (s, 3H). ^{13}C NMR (101 MHz, $DMSO-d_6$) δ 161.90, 136.40, 128.91, 128.79, 127.73, 124.70, 115.10, 113.09, 107.62, 55.39, 52.45, 49.07.

2.8 Synthesis of compound 7



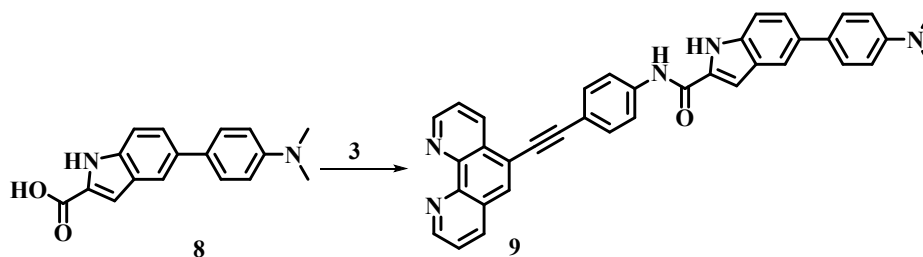
Compound **6** (0.13 g, 0.5 mmol) and 4-(dimethylamino) phenylboronic acid (0.12 g, 0.75 mmol) were dissolved in absolute ethanol (6 mL) and distilled water (2 mL). Then, palladium acetate (0.5 mol%) and anhydrous potassium carbonate (0.14 g, 1.0 mmol) were added to the mixed solution and reacted at room temperature. After the completion of the TLC monitoring reaction, the resulting solution was concentrated and the residue was diluted with water (30 mL). The mixture was extracted with EtOAc (3×50 mL) and the combined organic layer was washed with sat. salt water (2×30 mL), dried over anhydrous Na₂SO₄ and evaporated. The crude product was purified by a chromatographic column (PE/EA = 15:1) to obtain a yellow-green solid compound **7** (0.11 g, yield = 86%). ¹H NMR (400 MHz, DMSO-*d*₆) δ 12.04 – 11.76 (m, 1H), 8.10 – 7.71 (m, 1H), 7.63 – 7.38 (m, 4H), 7.17 (dd, *J* = 2.2, 0.9 Hz, 1H), 6.95 – 6.65 (m, 2H), 3.88 (s, 3H), 2.93 (s, 6H). ¹³C NMR (101 MHz, DMSO-*d*₆) δ 162.20, 149.83, 136.84, 133.45, 129.39, 127.87, 127.58, 124.35, 118.76, 113.32, 113.29, 108.46, 52.25, 40.65.

2.9 Synthesis of compound **8**



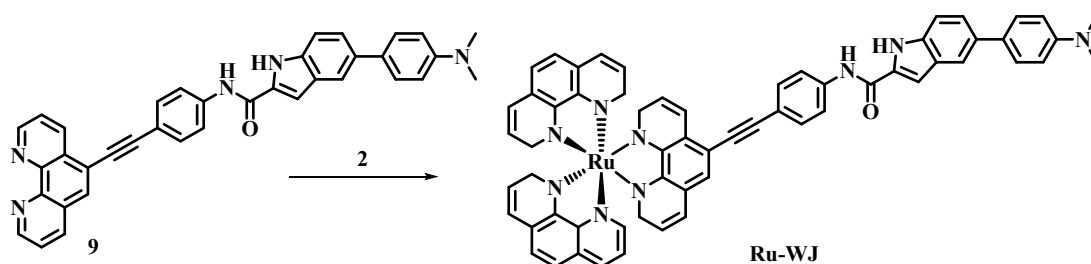
Compound **7** (0.11 g, 0.37 mmol) was dissolved in ethanol (8 mL) and 10% sodium hydroxide solution (4 mL), stirred at 70°C for 3 hours, and the reaction process was monitored by TLC. The mixture was cooled to room temperature, then adjusted the pH value to 2.0 with a hydrochloric acid solution (4 M), filtered and dried the filter residue to obtain a light yellow solid compound **8** (0.091 g, yield = 90%). ¹H NMR (400 MHz, DMSO-*d*₆) δ 11.80 (s, 1H), 7.88 (s, 1H), 7.66 (s, 2H), 7.52 (q, *J* = 8.7 Hz, 2H), 7.45 – 7.16 (m, 2H), 7.13 (d, *J* = 1.9 Hz, 1H), 3.03 (s, 6H).

2.10 Synthesis of compound **9**



Compound **8** (0.12 g, 0.50 mmol) and SOCl_2 (0.13 mL, 0.13 mmol) were dissolved in 10 mL of toluene, and the reaction mixture was reacted for 1 hour at reflux temperature. The mixture was cooled to room temperature and the solvent was removed to obtain the residue. Under the protection of N_2 , the flask containing the residue was cooled to 0°C , and compound **3** (0.15 g, 0.50 mmol) was dissolved in pyridine and added dropwise to the flask. The mixture was reacted overnight at room temperature, and then a brownish-black mixed solution was obtained by removing the solvent. It was recrystallized with ethanol, washed with water, and dried to obtain a red solid compound **9** (0.092 g, yield = 33%). $^1\text{H NMR}$ (400 MHz, $\text{DMSO}-d_6$) δ 9.15 (d, $J = 28.8$ Hz, 2H), 8.92 (d, $J = 8.3$ Hz, 1H), 8.56 (d, $J = 8.0$ Hz, 1H), 8.39 (s, 1H), 8.01 (d, $J = 8.6$ Hz, 2H), 7.82 (dd, $J = 15.8, 10.4$ Hz, 5H), 7.52 (q, $J = 8.4$ Hz, 5H), 6.82 (d, $J = 8.4$ Hz, 1H), 6.65 (d, $J = 8.4$ Hz, 1H), 3.18 (s, 3H), 2.94 (s, 3H). Mass spectrometry (ESI-HRMS, m/z): $[\text{M} + 1]^+$ calcd. for $[\text{C}_{37}\text{H}_{27}\text{N}_5\text{O} + 1]^+$: 558.2249; found: 558.2283.

2.11 Synthesis of compound Ru-WJ



Under argon protection, compound **2** (0.053 g, 0.10 mmol) and compound **9** (0.056 g, 0.10 mmol) were dissolved in MeOH (15 mL) and reacted in a condensing device for 7 hours. After the reaction, the obtained substance was purified by column chromatography with neutral Al_2O_3 ($\text{DCM}/\text{CH}_3\text{OH} = 50:1$) to obtain an orange-red

solid compound **Ru-WJ** (0.035 g, yield = 62%). Mass spectrometry (HRMS, m/z):
[M]⁺ calcd. for [C₆₁H₄₉N₉ORu]⁺: 1025.3098; found: 1025.5536.

3. Analysis and detection

3.1. Measurement of photophysical properties

The UV–Visible absorption spectra with a spectral range of 200-800 nm were recorded by the UH4150 spectrophotometer. The single photon emission spectrum was recorded by the RF6000 spectrophotometer (SHIMADZU).

3.2. Preparation of A β aggregates

A β 1-42 peptide (1 mg) (Chinese peptide) was dissolved in hexafluoro-2-propanol (HFIP, 1 mL) and divided into 10 PE tubes (100 μ L/tube). HFIP was removed by nitrogen flow, further dried with vacuum, and then stored at -80°C until use. HFIP-treated A β 1-42 (0.1 mg) was dissolved in 11 μ L DMSO and then diluted to 50 μ M with 434 μ L PBS buffer (pH = 7.4). At 37 °C, packaged A β 1-42 were incubated for 0, 1, and 7 days to obtain A β 1-42 monomers, oligomers, and fibrils. (The incubation results of A β 1-42 have been confirmed by DLS testing)

3.3. Quantum yield measurements

The quantum yields (QY) of **Ru-WJ** and **Ru-YH** ($\lambda_{\text{ex}} = 450$ nm, MeCN) were measured using Ru(bpy)₂⁺ 3as standard ($\lambda_{\text{ex}} = 450$ nm, MeCN, $\Phi = 0.018$ %). Quantum yields were calculated using equation (1), where Φ_f^i and Φ_f^s are the photoluminescence QY of the sample and the standard, respectively; F^i and F^s are the integrated intensities (areas) of sample and standard spectra, respectively; f_x is the absorption factor, the fraction of the light impinging on the sample that was absorbed ($f_x = 1 - 10^{-A_x}$, A = absorbance); the refractive indices of the sample and reference solution are n_i and n_s , respectively.

$$\Phi_f^i = \frac{F^i f_s n_i^2}{F^s f_i n_s^2} \Phi_f^s \quad (1)$$

3.4. The determination of pKa .

DI waters with pH = 1-14 were obtained by constant modulation of DI water with 0.1 M solutions of NaOH and HCl. The pH values were measured with a pH meter (Mettler Toledo, FiveEasy Plus). **Ru-WJ** and **Ru-YH** were dissolved in water with

different pH values. The fluorescence spectrum of **Ru-WJ** (10 μM , $\lambda_{\text{ex}} = 450 \text{ nm}$) and **Ru-YH** (10 μM , $\lambda_{\text{ex}} = 427 \text{ nm}$) were recorded by RF6000 spectrophotometer. pK_a was obtained by fitting the Boltzmann curve with the maximum fluorescence intensity (Y-axis) plotted against pH (X-axis).

3.5. Log P_{ow} determination.

The log P_{ow} determination of **Ru-WJ** and **Ru-YH** were conducted using the shake-flask method. **Ru-WJ** and **Ru-YH** (10 μM) were dissolved in DI water. Subsequently, the solution was added to an equal volume of 1-octanol which was saturated by water, shaken vigorously at 37 °C for 24 h, and centrifuged for 10 min to achieve phase separation. The initial and final concentrations of compounds in the aqueous phase were determined by the UV–Visible spectrum method, and the 1-octanol-water partition coefficients (log P_{ow}) were calculated.

Due to the fact that log P_{ow} depends on the distribution of molecules in both organic and aqueous phases. From the perspective of molecular structure, there are significant differences in the size and dipole moment of **Ru-WJ** and **Ru-YH** molecules themselves. Due to the relationship between molecular volume and molecular weight, it also affects the size of the solvent cavity formed by dissolving molecules. The dipole moment affects the polar arrangement of molecules and solvents.^{3, 4}

3.6 Molecular docking

In this study, the two molecules **Ru-WJ** and **Ru-YH** were sketched and optimized by SYBYL-X 2.1. The optimizations of them were performed using Gasteiger-Hückel charges by the Tripos force field with a gradient of 0.005 and a maximum iteration number of 1000. The other parameters were set as default. Then the two molecules were docked into the receptor respectively after generating the docking pocket and adjusting the docking protocol by the Surflex-Dock Geom module in SYBYL-X 2.1. And the ligand conformation possessing the highest docking score of each compound was picked for further analysis of the binding mode. The visualization of the docking results was obtained by PyMOL. Besides, binding free energies (kcal/mol) normally reflect the binding affinities of ligands to the receptor and can be calculated in combination with the total scores of the dockings by the formulas below (2, 3), in which K_d refers to a

dissociation constant of a ligand and RT equals 0.59 kcal/mol.

$$\text{Total Score} = -\lg K_d \quad (2)$$

$$\Delta G = RT * \ln K_d \quad (3)$$

The X-ray crystal structure of macrocyclic β -sheet peptides shows that all these peptides are assembled into triangular trimers in a similar manner, which may further assemble into higher-order oligomers such as hexamers and dodecamers.⁵⁻⁷ And macrocyclic peptides can selectively recognize different types of $A\beta$. Among them, 4NTR contains two heptapeptide β -Strands $A\beta$ 17-23 (or $A\beta$ 16-22) and $A\beta$ 30-36 locked in an antiparallel β - Sheet by two δ - Linked orphanine β - Turn mimics (δ Orn). Additionally, the working model demonstrates exceptional stability and high resolution, while also encompassing potential binding sites for the proposed docked molecules. Consequently, protein 4NTR has been identified as the optimal candidate for conducting molecular docking experiments.

3.7 Fluorescence spectral measurements of Ru-WJ and Ru-YH with $A\beta$ 1-42 oligomers/fibrils

$A\beta$ 1-42 peptide (1 mg) (Chinese peptide) was dissolved in hexafluoro-2-propanol (HFIP, 1 mL) and divided into 10 PE tubes (100 μ L/tube). HFIP was removed by nitrogen flow, further dried with vacuum, and then stored at -80°C until use. HFIP-treated $A\beta$ 1-42 (0.1 mg) was dissolved in 11 μ L DMSO and then diluted to 50 μ M with 434 μ L PBS buffer (pH = 7.4). At 37 $^\circ\text{C}$, packaged $A\beta$ 1-42 were incubated for 0, 1, and 7 days to obtain $A\beta$ 1-42 monomers, oligomers, and fibrils. (The incubation results of $A\beta$ 1-42 have been confirmed by DLS testing)

Ru-WJ and **Ru-YH** (10 μ M) were incubated with varying concentrations of $A\beta$ 1-42 oligomers (1-18 μ M)/fibrils (1-16 μ M) at 37 $^\circ\text{C}$ for 30 min. The emission spectra of **Ru-WJ** ($\lambda_{\text{ex}} = 450$ nm) and **Ru-YH** ($\lambda_{\text{ex}} = 454$ nm) were recorded using a FLS1000 spectrophotometer (Edinburgh Instruments).

3.8. Determination of the binding constant of Ru-WJ and Ru-YH for $A\beta$ 1-42 aggregates

The recognition of amyloid- β ($A\beta$) is a challenging task for the early diagnosis of

neurodegenerative diseases, for example, Alzheimer's disease. A β 1-42 contains 42 amino acids, which are Asp-Ala-Glu-Phe-Arg-His-Asp-Ser-Gly-Tyr-Glu-Val-His-His-Gln-Lys-Leu-Val-Phe-Phe-Ala-Glu-Asp-Val-Gly-Ser-Asn-Lys-Gly-Ala-Ile-Ile-Gly-Leu-Met-Val-Gly-Gly-Val-Val-Ile-Ala. And the peptide sequence Lys-Leu-Val-Phe-Phe (KLVFF) is considered to be the main driving factor for A β fibrillation. It not only has good lipophilicity, but also is a specific ligand for A β , which can cooperate with the red blood cell membrane to selectively capture A β and inhibit its aggregation.^{1, 2} Here, it is used as the targeted part of the probe **Ru-YH** in molecular design.

A β 1–42 oligomer and fibrils (2 μ M final concentration) were mixed with various concentrations of **Ru-WJ** and **Ru-YH** (2-20 μ M) in PBS (pH = 7.4). The K_d was determined as described previously by fitting the data to a one-site specific binding algorithm: $Y = B_{\max} * X / (K_d + X)$, where X is the concentration of the probe, Y is the specific binding fluorescence intensity, and B_{\max} corresponds to the apparent maximal observable fluorescence upon binding of probes to aggregated A β ₁₋₄₂ oligomer or fibrils. The K_d binding curve was generated by GraphPad Prism 8 with nonlinear one-site binding regression.

3.9. Stability of Ru-WJ and Ru-YH

Ru-WJ and **Ru-YH** were dissolved in PBS (5% DMSO, pH = 7.4) to a final concentration of 10 μ M. The emission spectra of **Ru-WJ** (λ_{ex} = 450 nm) and **Ru-YH** (λ_{ex} = 454 nm) were recorded using a FLS1000 spectrophotometer (Edinburgh Instruments) at different times (0-24 h). Maximum intensity wavelengths were plotted against time.

3.10. Selectivity of Ru-WJ and Ru-YH

Ru-WJ and **Ru-YH** (10 μ M) were added to 5 μ M of cysteine (Cys), glycine (Gly), glutathione (GSH), histidine (His), arginine (Arg), lysine (Lys), serine (Ser), phenylalanine (Phe), human serum albumin (HSA), hemoglobin (HGB), Zn²⁺, Cu²⁺, Mg²⁺, K⁺, Fe²⁺, Na⁺, Ca²⁺, A β monomers, A β oligomers, and A β fibrils to the PBS solution, respectively. After co-incubation for 30 min, the emission spectra of **Ru-WJ** and **Ru-YH** in different centrifuge tubes were tested.

3.11. Cell culture and Cytotoxicity.

Cells were seeded at a density of 1×10^4 cells/well in a 96-well plate in prepared medium (100 μ L) supplemented for 24 hours. Then, the desired concentration of **Ru-WJ** and **Ru-YH** were added. After 24 hours of incubation, the spent medium was aspirated with a syringe and the cells were washed with PBS. Then 20 μ L/well MTT and 200 μ L medium was added and incubated for 4 h. Then, the medium was aspirated, and 150 μ L DMSO was added. The absorbance value of each well was measured at 490 nm with a Thermo Scientific microplate reader. Each concentration of our probe was measured in four independent experiments. Relative cell viability was calculated by the following equation (4):

$$\text{Cell viability (\%)} = \frac{OD \text{ treated} - OD \text{ background}}{OD \text{ control}} \times 100\% \quad (4)$$

3.12. TEM observation and DLS examination of A β 1-42 peptides, oligomers, and fibrils.

All A β 1-42 sample solutions (5 μ M) were prepared from 50 μ M stock solutions in PBS buffer. A β 1-42 sample solution was incubated with **Ru-WJ**, **Ru-YH**, or Curcumin (25 μ M) for 0 day, 1 day, and 7 days.

TEM: 8 μ L of the diluted A β 1-42 sample solution was dropped onto a carbon-coated copper grid (T200H-Cu Electron Microscopy Science, Washington, USA) for 30 min, and washed with DI water for 1 min. The A β 1-42 samples were then negatively stained with 2% uranyl acetate for 5 min and then washed with DI water for 1 min. The stained samples were then dried overnight. Transmission electron microscopy images were acquired under a TECNAI G2 20 S-TWIN transmission electron microscope at an accelerating voltage of 200 kV, a point resolution of 0.248 nm, and a line resolution of 0.144 nm.

DLS: Particle size analysis data of 1 mL incubated or non-incubated A β 1-42 sample solutions were obtained from the Malvern Zetasizer ZS90.

3.13. *Ex vivo* brain imaging

Brain sections were obtained from APP/PS1 transgenic mice (C57BL6, APP/PS1, 2.5/8 months old, male) and age-matched wild-type mice. After the mice were sacrificed, the brains were covered with Neg-50 cryo-embedding medium. The embedded tissue was then cut into serial sections (40 μm in thickness) in a CryoStar NX50 cryostat, and the sections were co-stained with **Ru-WJ** (100 μM , $\lambda_{\text{ex}} = 458 \text{ nm}$, $\lambda_{\text{em}} = 620 \text{ nm}$), **Ru-YH** (100 μM , $\lambda_{\text{ex}} = 458 \text{ nm}$, $\lambda_{\text{em}} = 620 \text{ nm}$) and ThS ($\lambda_{\text{ex}} = 488 \text{ nm}$, $\lambda_{\text{em}} = 550 \text{ nm}$). Coverslips were finally mounted and the slides were imaged by a confocal laser scanning microscope (Carl Zeiss LSM880).

3.14. Brain homogenate experiment and *in vivo* imaging

APP/PS1 transgenic mice (C57BL6, APP/PS1, 2.5-months old, male) and age-matched wild-type mice were shaved and injected intravenously with **Ru-WJ** and **Ru-YH**. **Ru-WJ** and **Ru-YH** (2 mg/kg, $\lambda_{\text{ex}} = 465 \text{ nm}$, $\lambda_{\text{em}} = 620 \text{ nm}$) were injected intravenously, respectively. The brains were taken out after the mice were sacrificed. Then the brain tissue proteins were obtained by grinding. The optical images were acquired using an exposure time of 500 μs . During imaging, the mice were anesthetized with 2% isoflurane gas (3.0 L/min) in an oxygen flow. Imaging data were analyzed by Living Image Software.

4. Supporting Figures

4.1. UV-vis spectra in PBS

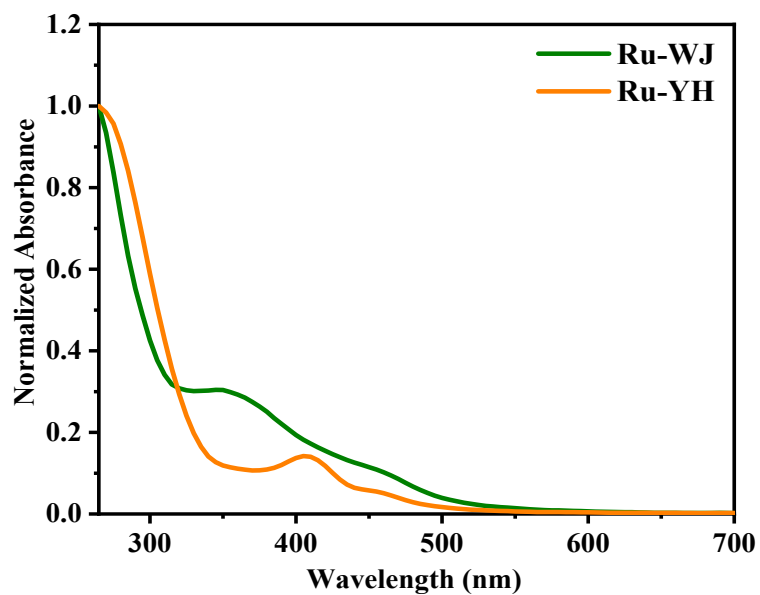


Fig. S1. Normalized UV-Visible absorbance spectra of **Ru-WJ** ($\lambda_{\text{abs}} = 450$ nm) and **Ru-YH** ($\lambda_{\text{abs}} = 454$ nm) (10 μM) in PBS.

4.2. Spectroscopic studies of the probes versus pH

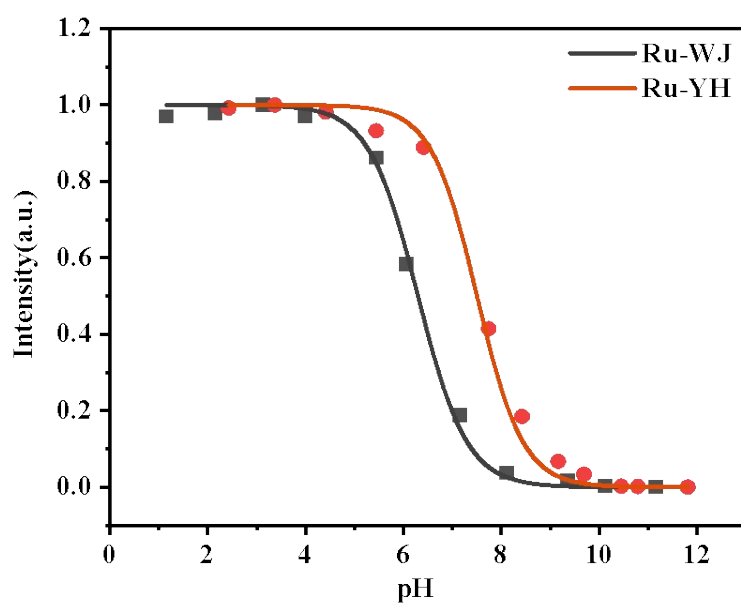


Fig. S2. Nonlinear fitting of the fluorescence intensity of **Ru-WJ** ($\lambda_{\text{ex}} = 450$ nm) and **Ru-YH** ($\lambda_{\text{ex}} = 427$ nm) in various pH values (5% DMSO in distilled water).

4.3. Chemical stability

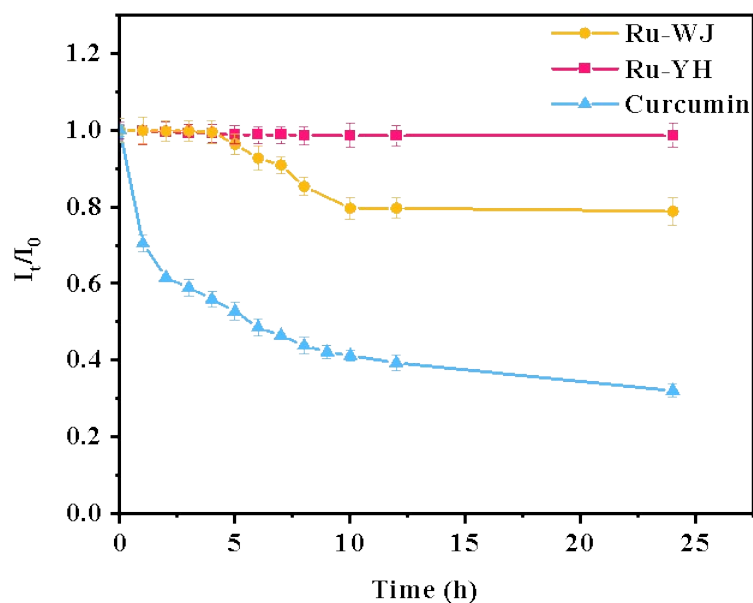


Fig. S3. Chemical stability of **Ru-WJ** and **Ru-YH** (10 μ M) in PBS. (5% DMSO, pH = 7.4, 25 $^{\circ}$ C)

4.4. Molecular docking analysis

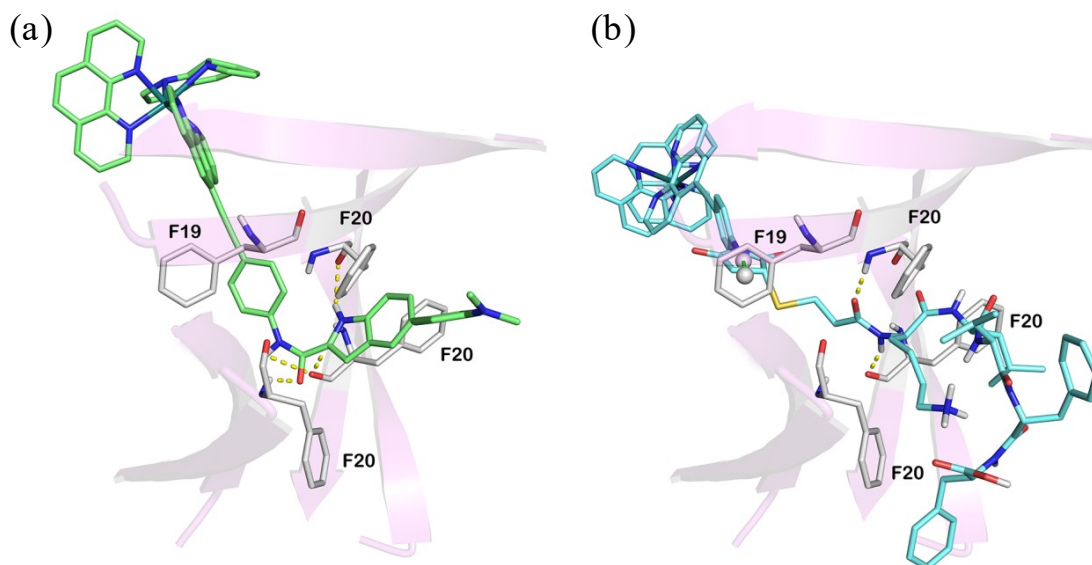


Fig. S4. The docking results of compounds **Ru-WJ** (a) and **Ru-YH** (b) with the A β oligomer (PDB code: 4NTR). Hydrogen bonds and π - π stacking interactions were exhibited as yellow and green dashes.

4.5. The selectivity of Ru-WJ and Ru-YH

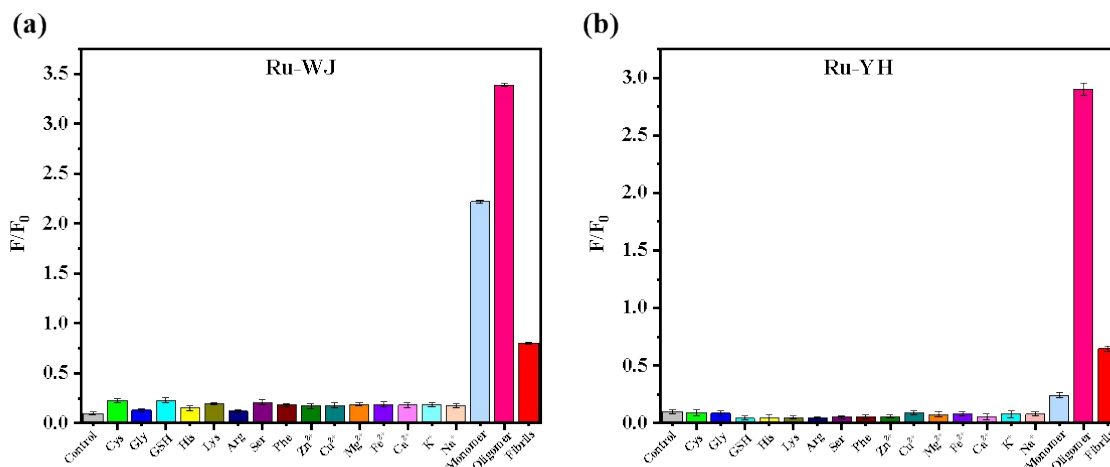


Fig. S5. High selectivity toward potential competitive species and A β 1-42 aggregates. The fluorescent spectral response of (a) **Ru-WJ** and (b) **Ru-YH** (10 μ M) towards A β 1-42 aggregates, metal ions and amino acid (5.0 μ M) in PBS (pH = 7.4).

4.6. Binding affinity

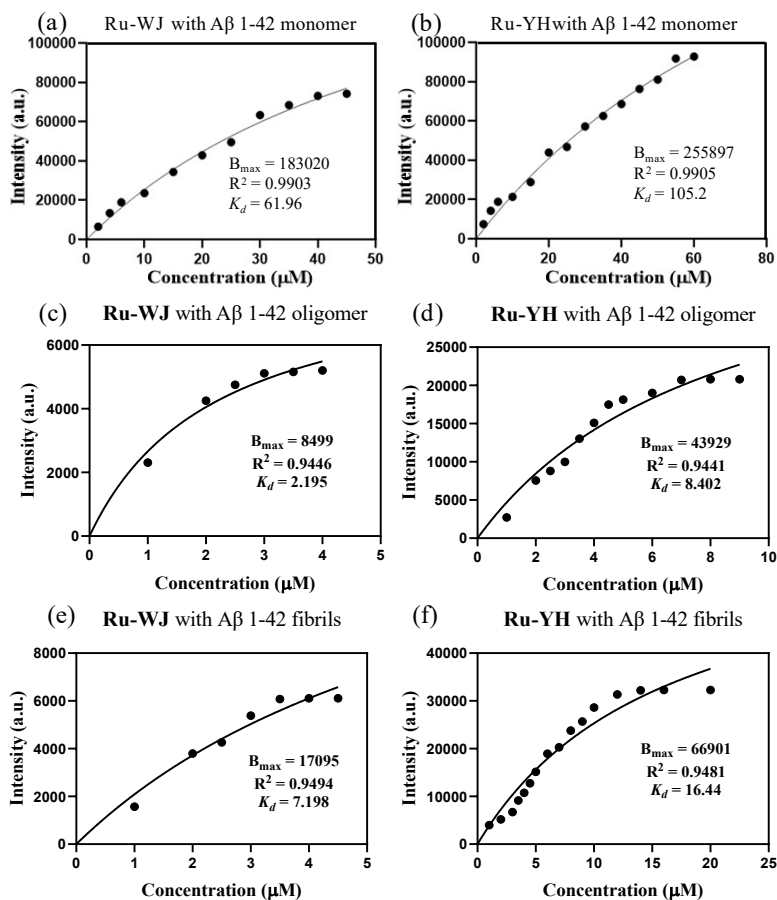


Fig. S6. Plot of the difference in fluorescence intensity (ΔF) as a function of the

concentration of (a, c, e) **Ru-WJ** ($\lambda_{\text{ex}} = 450 \text{ nm}$) and (b, d, f) **Ru-YH** ($\lambda_{\text{ex}} = 454 \text{ nm}$) in the presence of A β monomer, oligomer or fibrils (2 μM) in PBS solution (1% DMSO, pH = 7.4).

4.7. The MTT assay of Ru-WJ and Ru-YH

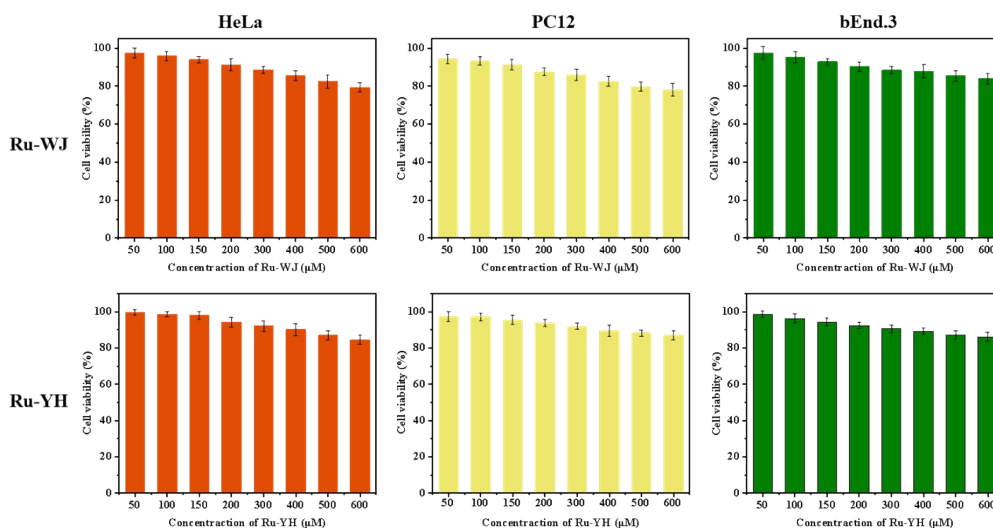


Fig. S7. Cell viability after incubation of **Ru-WJ** and **Ru-YH** at different concentrations with HeLa, PC12 and bEnd.3 cell by MTT assay, at 37°C for 24 h.

4.8. ^1H NMR, ^{13}C NMR, HPLC, HRMS and Infrared spectrum

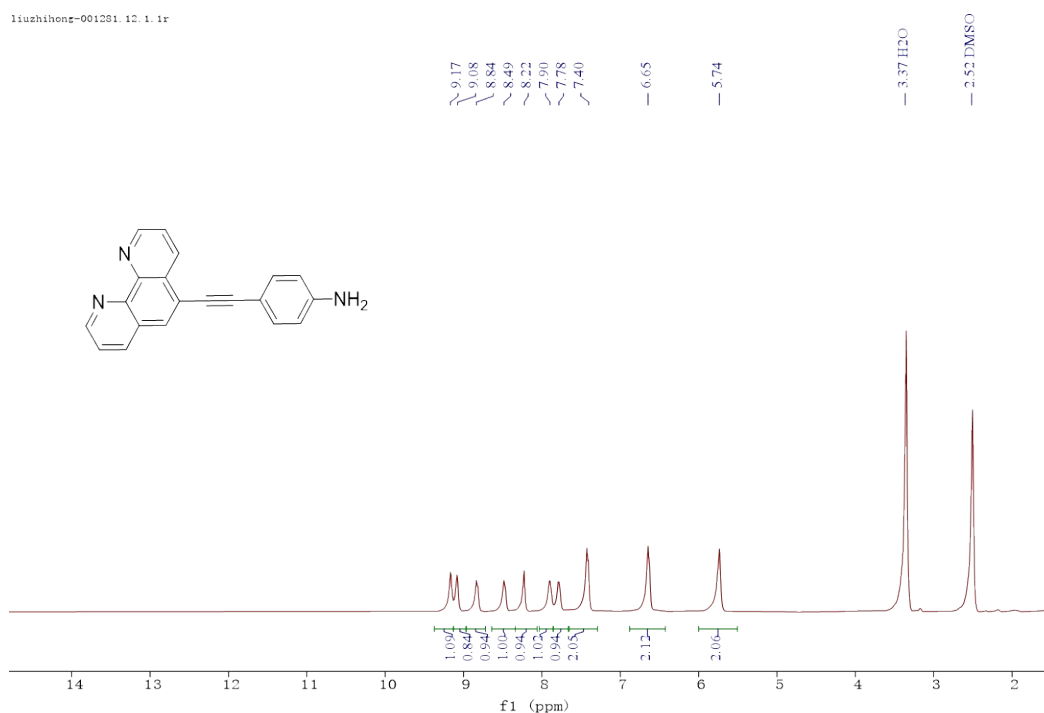


Fig. S8. ^1H NMR spectrum of compound **3** in CDCl_3 .

liuzhihong-001819-C13. 20. 1. 1r

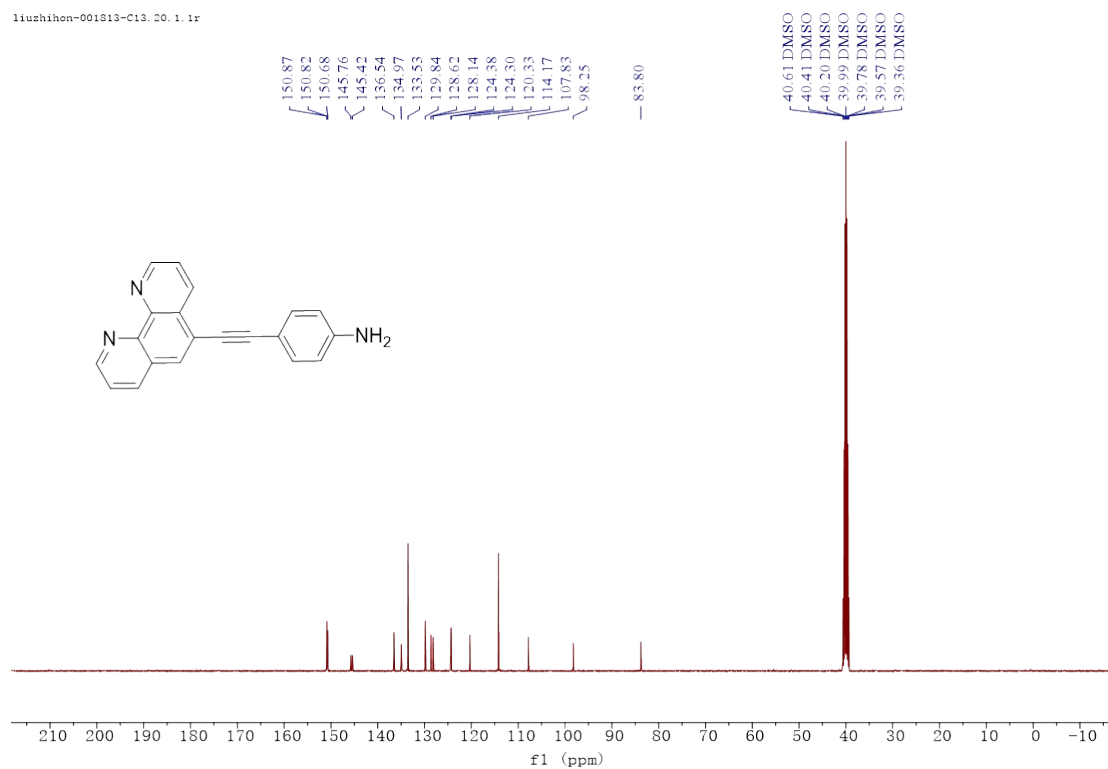


Fig. S9. ¹³C NMR spectrum of compound **3** in DMSO-*d*₆.

liuzhihong-001811. 10. 1. 1r

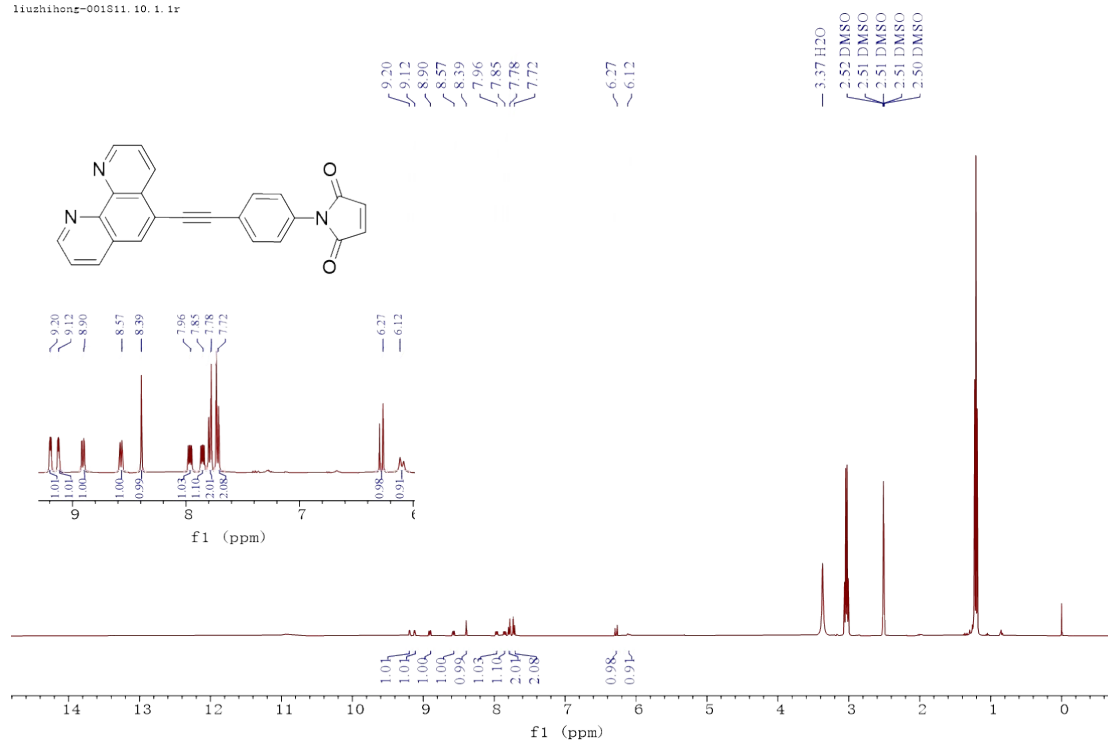


Fig. S10. ¹H NMR spectrum of compound **4** in DMSO-*d*₆.

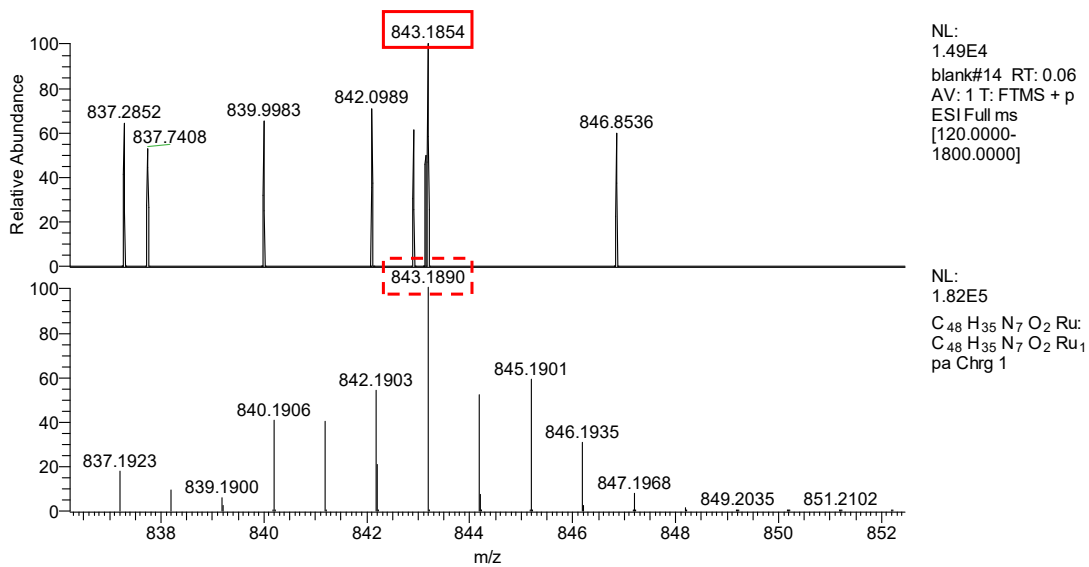


Fig. S11. HRMS spectrum of compound **5**.

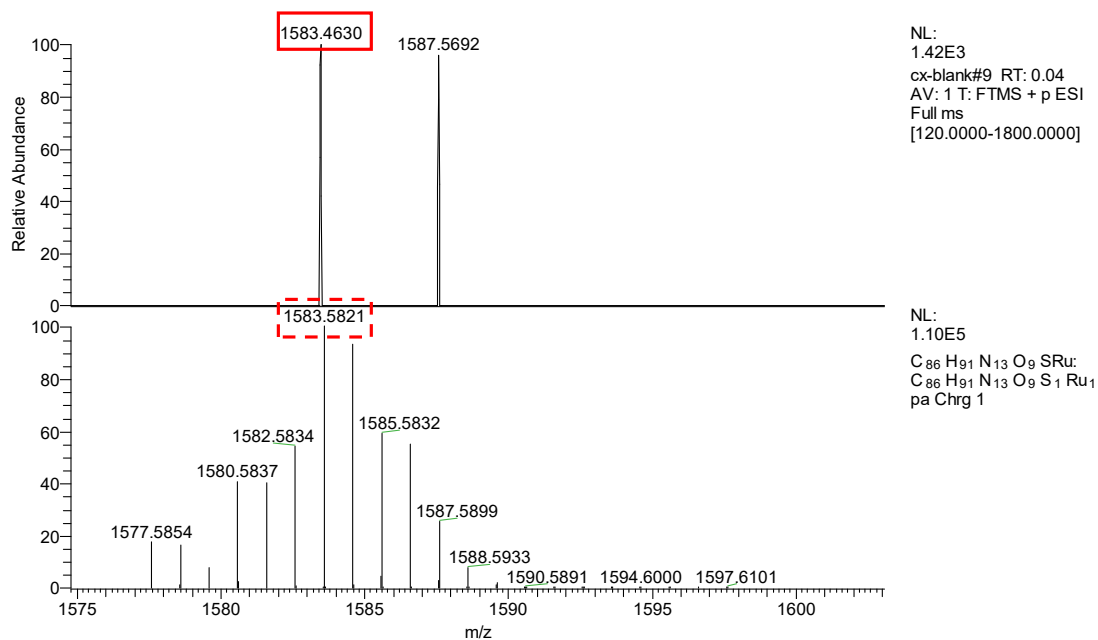
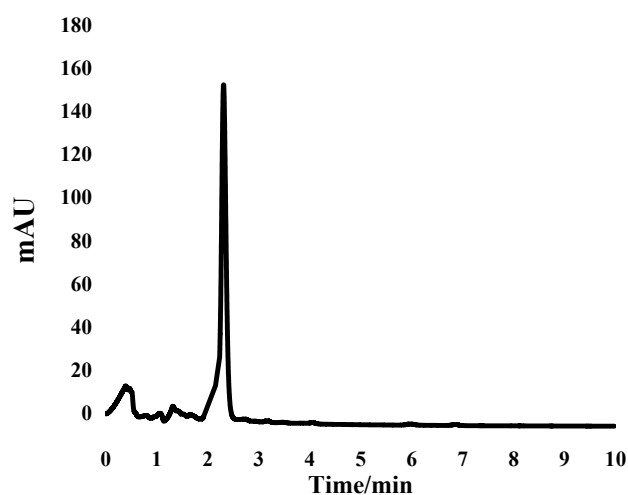


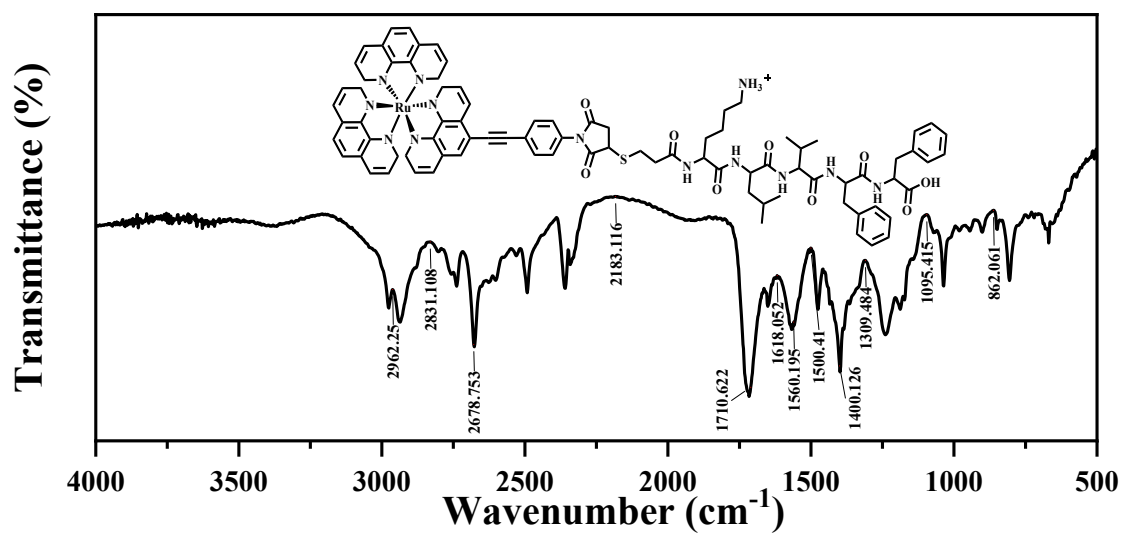
Fig. S12. HRMS spectrum of compound **Ru-YH**.



Column: YWG C18 250 × 4.6 mm; eluent: MeOH = 100; flow rate: 1.5 mL/min; detector: UV-650 nm.

Peak#	Ret. Time (min)	Area	Area (%)
1	0.389	170.011	9.690
2	0.461	101.959	5.811
3	1.060	28.729	1.637
4	1.316	99.090	5.648
5	1.650	36.383	2.074
6	2.308	1263.698	72.026
7	2.720	27.405	1.562
8	3.162	13.018	0.742
9	4.050	3.604	0.205
10	5.963	6.242	0.358
11	6.852	4.368	0.249

Fig. S13. HPLC spectra of compound **Ru-YH**.




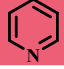
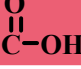
		C-S	C-N	C=O	N-H		C≡C	C-H
1500.41 cm ⁻¹	1618.05 cm ⁻¹	1095.41 cm ⁻¹	1309.48 cm ⁻¹	1710.62 cm ⁻¹	2962.25 cm ⁻¹	2678.75 cm ⁻¹	2183.12 cm ⁻¹	2831.11 cm ⁻¹

Fig. S14. Infrared spectra of compound **Ru-YH**.

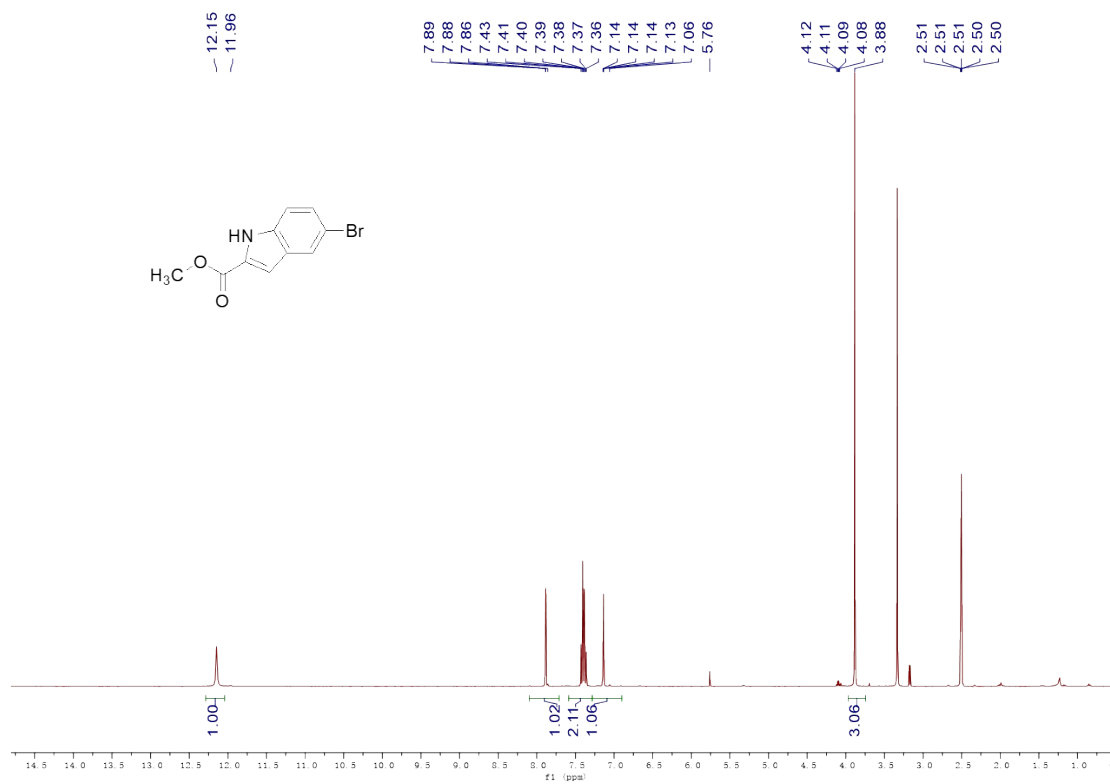


Fig. S15. ¹H NMR spectrum of compound **6** in DMSO-*d*₆.

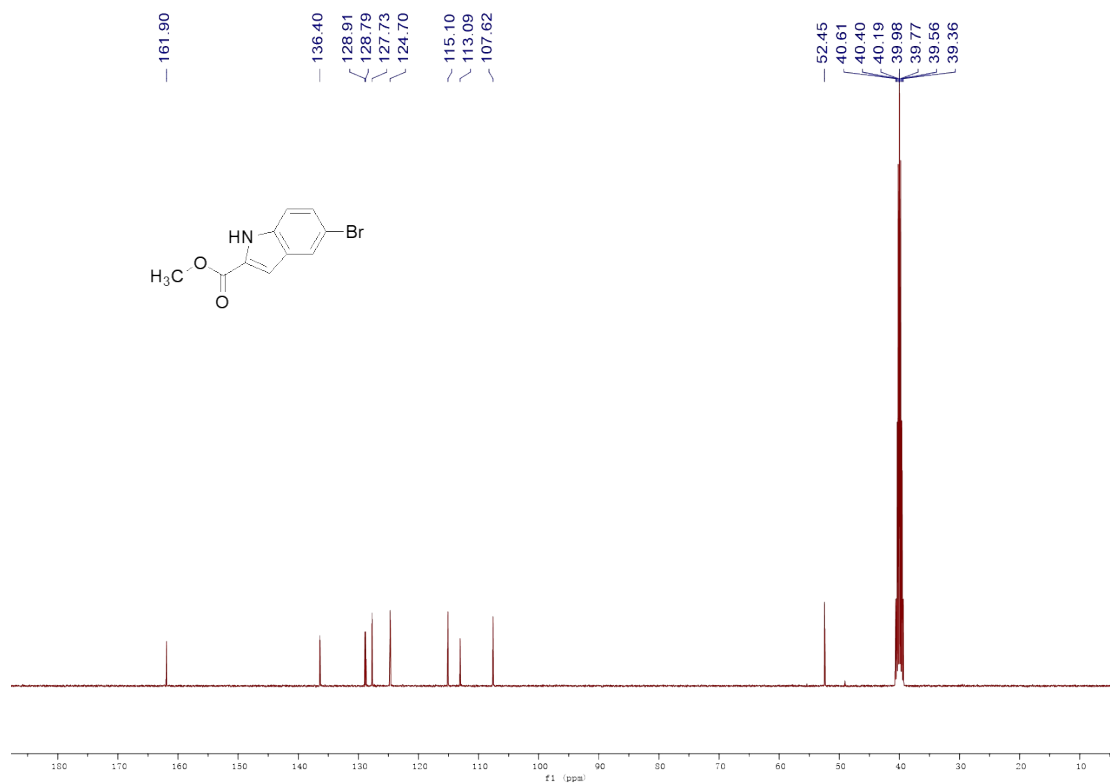


Fig. S16. ¹³C NMR spectrum of compound **6** in DMSO-*d*₆.

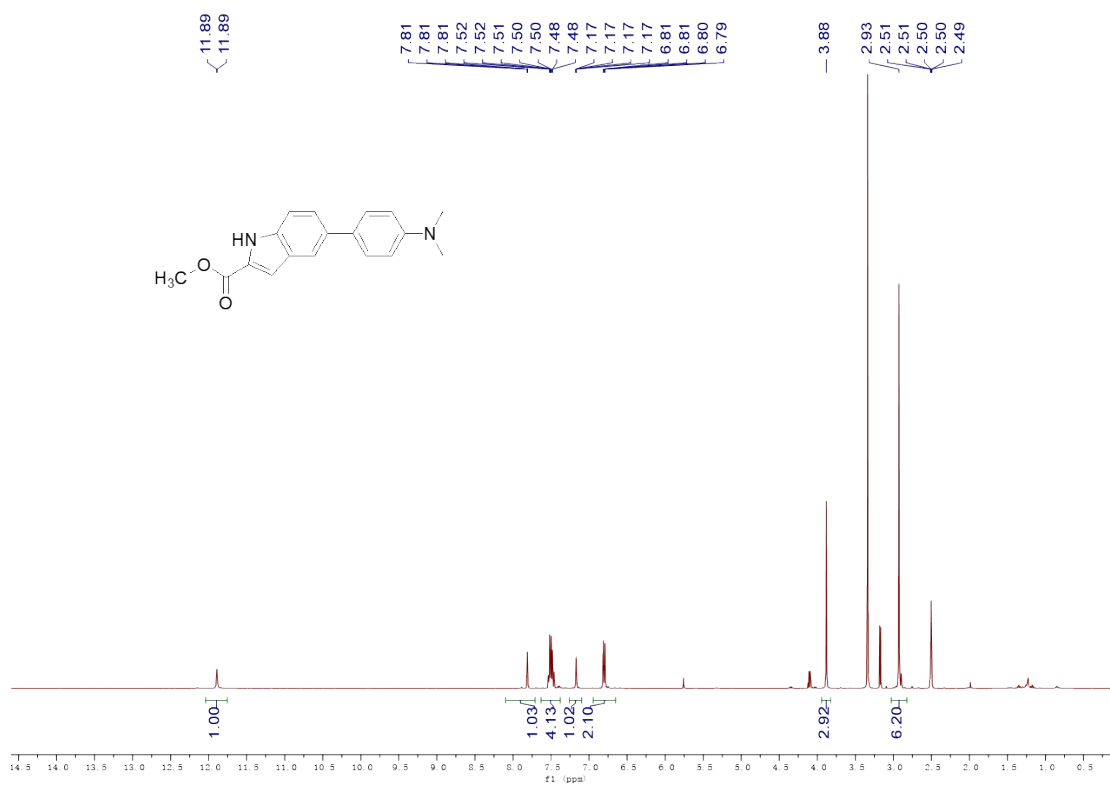


Fig. S17. ¹H NMR spectrum of compound **7** in DMSO-*d*₆.

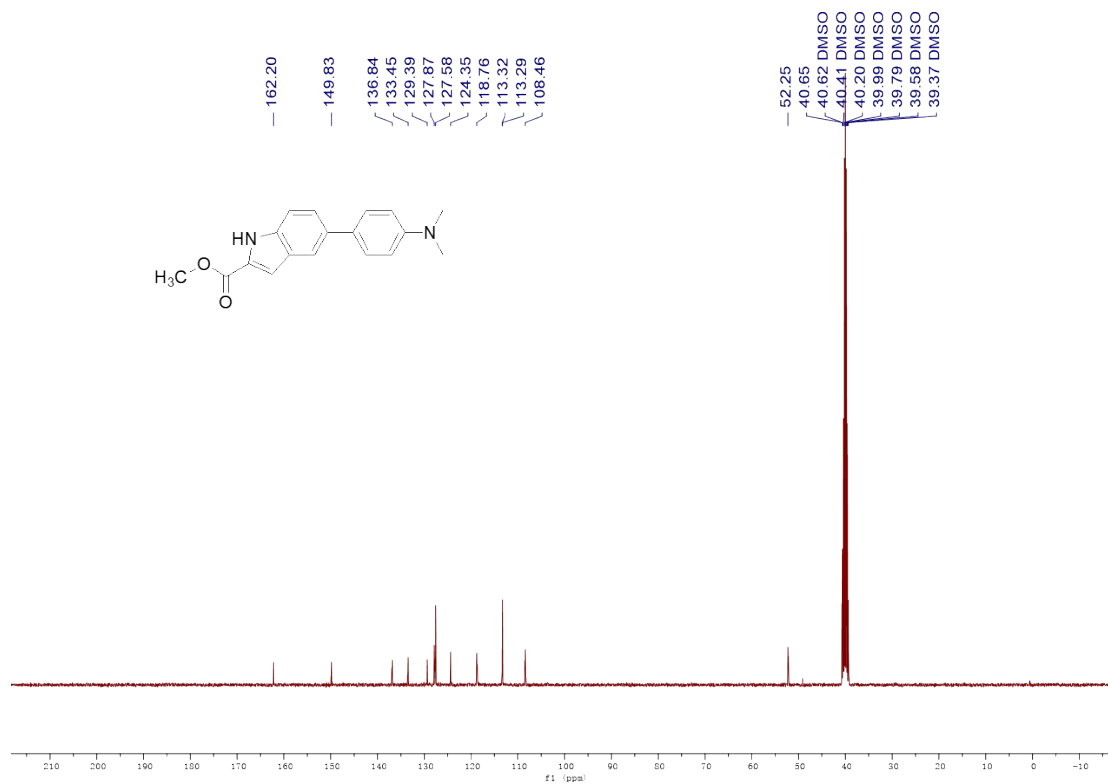


Fig. S18. ¹³C NMR spectrum of compound **7** in DMSO-*d*₆.

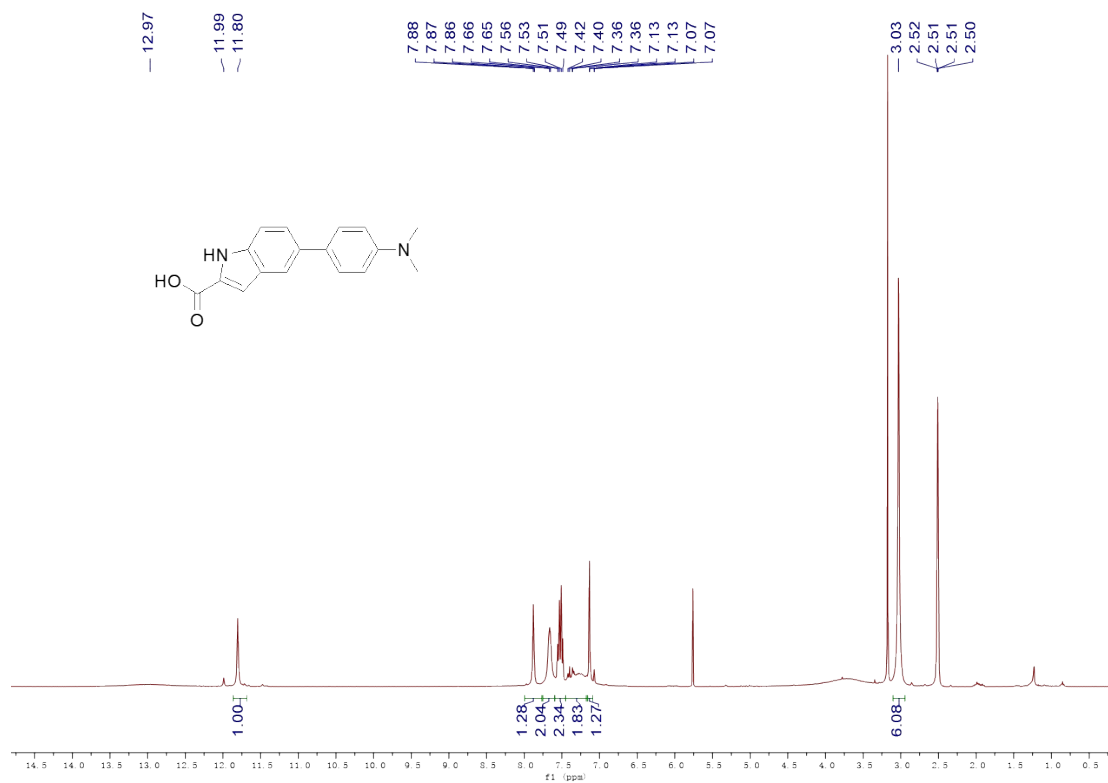


Fig. S19. ¹H NMR spectrum of compound **8** in DMSO-*d*₆.

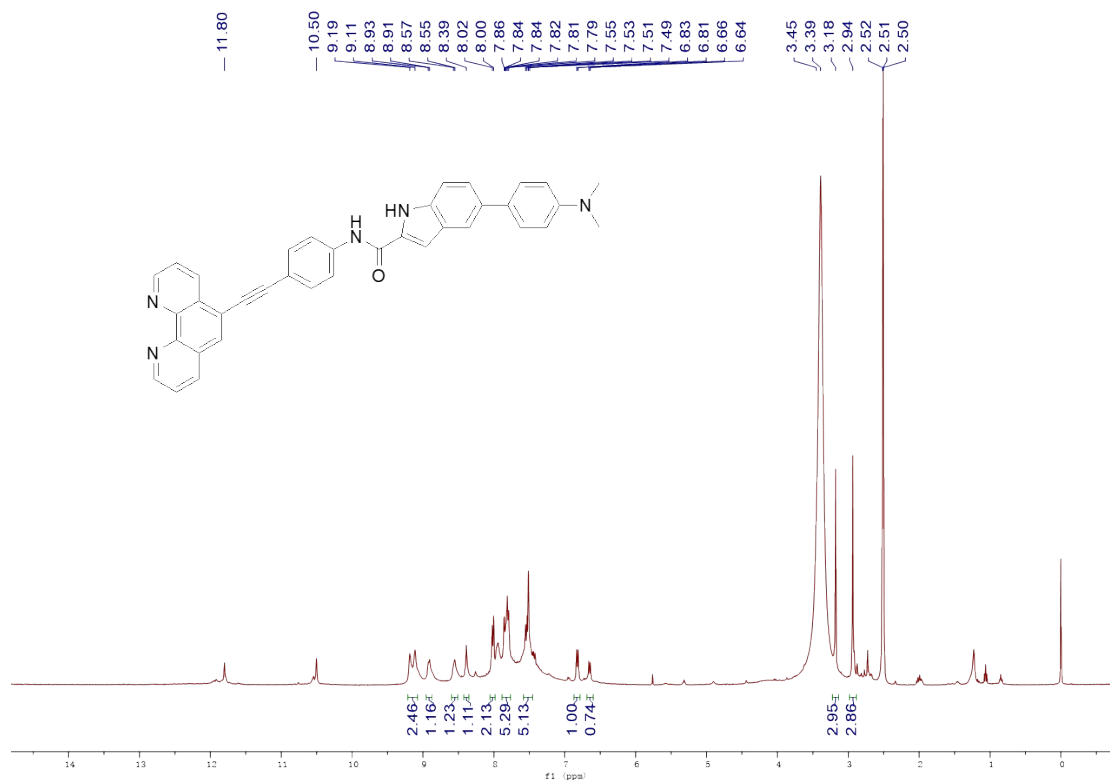


Fig. S20. ¹H NMR spectrum of compound **9** in DMSO-*d*₆.

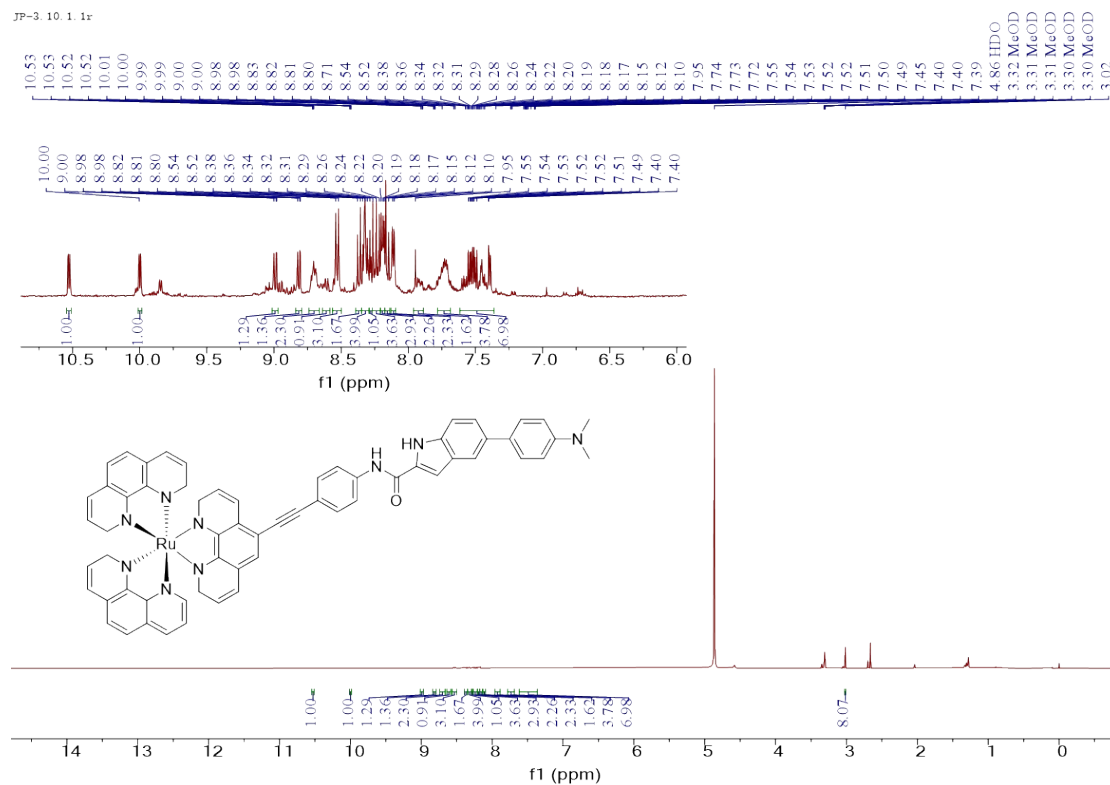


Fig. S21. ¹H NMR spectrum of compound **Ru-WJ** in MeOD.

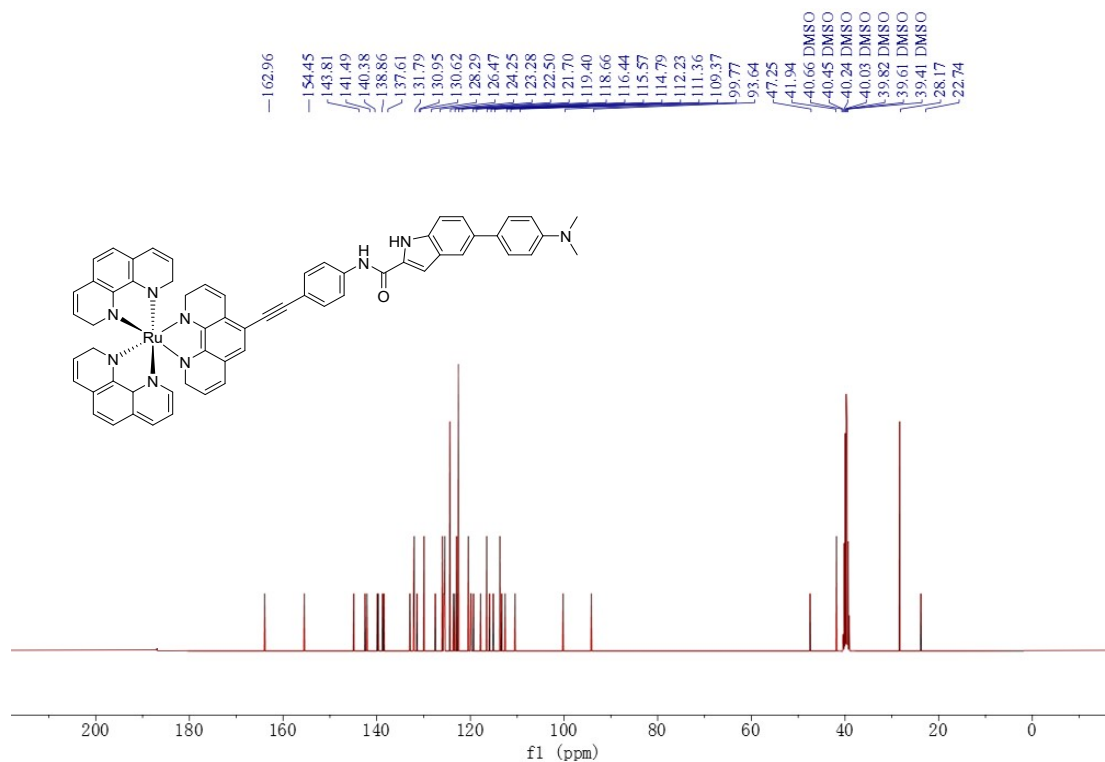


Fig. S22. ¹³C NMR spectrum of compound **Ru-WJ** in DMSO-*d*₆.

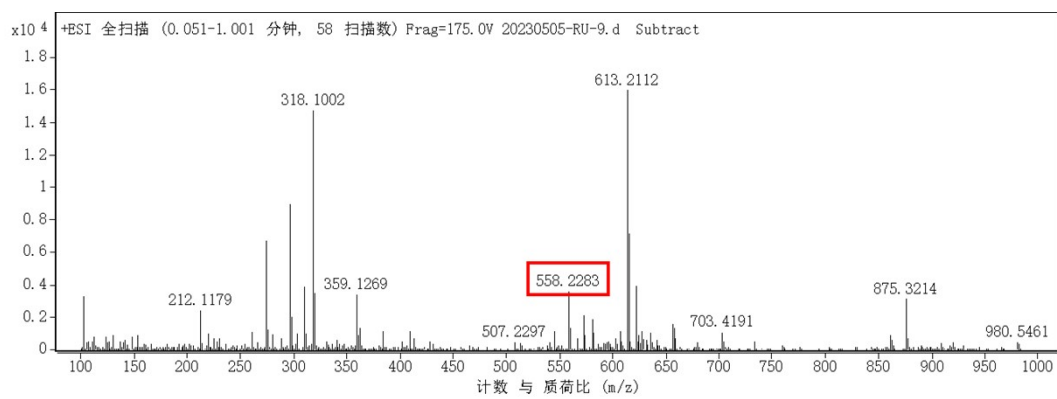


Fig. S23. ESI-HRMS spectrum of compound **9**.

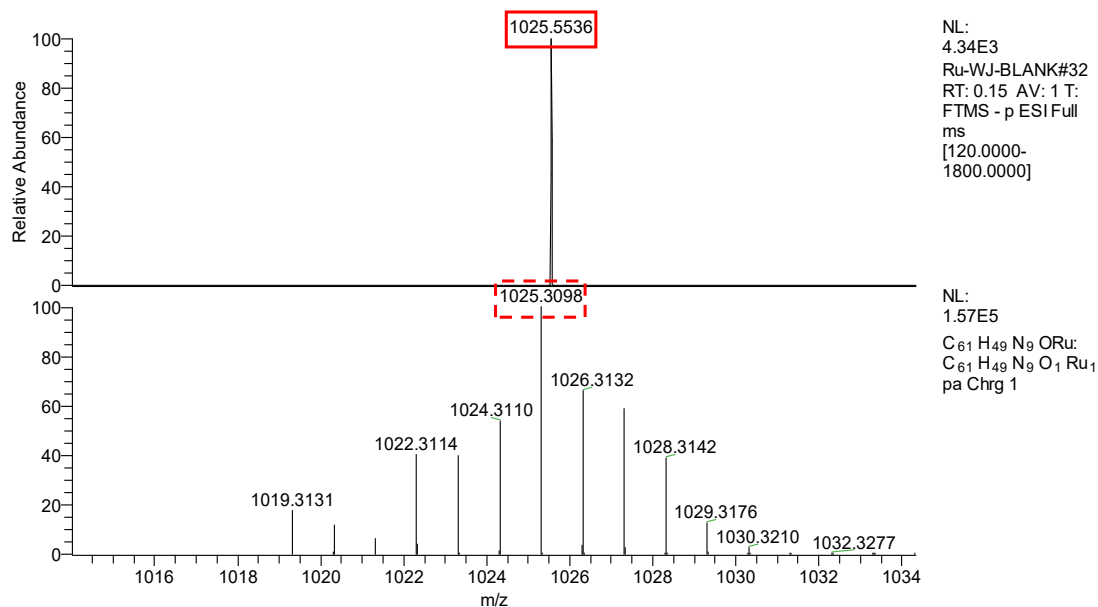
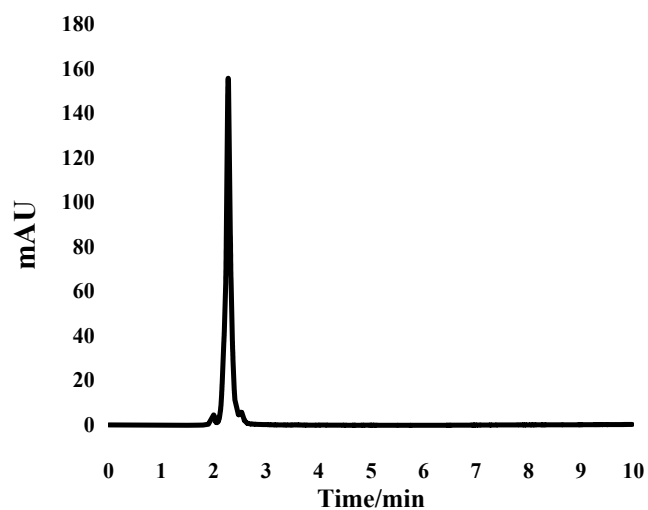


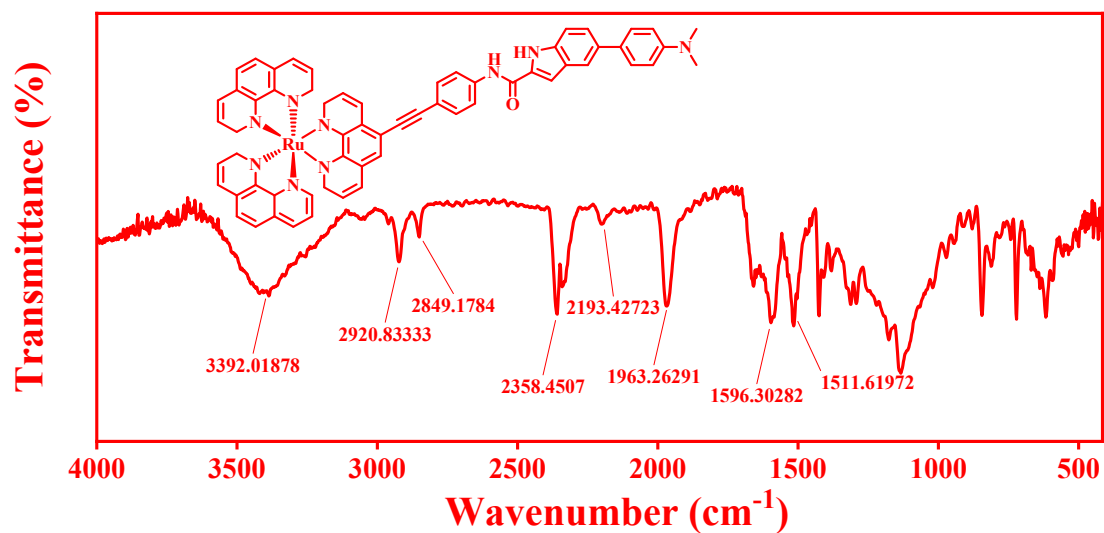
Fig. S24. HRMS spectrum of compound **Ru-WJ**.



Column: YWG C18 250 × 4.6 mm; eluent: MeOH = 100; flow rate: 1.5 mL/min; detector: UV-650 nm.

Peak#	Ret. Time (min)	Area	Area (%)
1	2.004	18.578	1.677
2	2.276	1054.852	95.261
3	5.578	33.893	3.061

Fig. S25. HPLC spectra of compound **Ru-WJ**




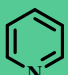
		C-N	C=O	N-H	CH ₃	C≡C	C-H
1511.62 cm ⁻¹	1596.30 cm ⁻¹	1132.06 cm ⁻¹	1658.56 cm ⁻¹	3392.02 cm ⁻¹	2920.83 cm ⁻¹	2193.43 cm ⁻¹	2849.18 cm ⁻¹

Fig. S26. Infrared spectra of compound **Ru-WJ**.

5. References

1. Antonino M.; Giuseppe D. N.; Rita T.; , Angela S.; , Giuseppe S.; Anna P.; Maria P. C.; Alberto R.; Maria L. G.; Placido G. M.; Valentina V.; Norberto M.; Giuseppe P. KLVFF oligopeptide-decorated amphiphilic cyclodextrin nanomagnets for selective amyloid beta recognition and fishing. *J. Colloid Interf. Sci.* **2022**, *613*, 814-826.
2. Liu D.; Fu D.; Zhang L.; Sun L. Detection of amyloid-beta by Fmoc-KLVFF self-assembled fluorescent nanoparticles for Alzheimer's disease diagnosis. *Chinese Chem. Lett.* **2021**, *32*, 1066-1070.
3. Hansch C.; Leo A.; Mekapati S. B.; Kurup A. QSAR and ADME. *Bioorgan. Med. Chem.* **2004**, *12*, 3391-3400.
4. Aliagas I.; Gobbi A.; Lee M. L.; Sellers B. D. Comparison of logP and logD correction models trained with public and proprietary data sets. *Comput. Aid. Mol. Des.* **2022**, *36*, 253-262.
5. Firouzi R.; Noohi B. Identification of key stabilizing interactions of amyloid- β oligomers based on fragment molecular orbital calculations on macrocyclic β -hairpin peptides. *Proteins.* **2022**, *90*, 229-238.
6. Teoh C. L.; Su D.; Sahu S.; Yun S. W.; Drummond E.; Prelli F.; Lim S.; Cho S.; Ham S.; Wisniewski T.; Chang Y. T. A Chemical Fluorescent Probe for the Detection of A β Oligomers. *J. Am. Chem. Soc.* **2015**, *137*, 13503-13509.
7. Lv G.; Sun A.; Wei P.; Zhang N.; Lan H.; Yi T. A spiropyran-based fluorescent probe for the specific detection of b-amyloid peptide oligomers in Alzheimer's disease. *Chem. Commun.* **2016**, *52*, 8865-8868.